# Using an Uncalibrated Camera for Undistorted Projection over a Mobile Region of Interest

Mamona Awan*
National University of Computer and Emerging Sciences – FAST,
Lahore, 54700 PAKISTAN

Kwang Hee Ko†
Gwangju Institute of Science and Technology
Gwangju, 61005 REPUBLIC OF KOREA

**Abstract**

This paper presents a system for projection over a mobile region of interest. The region is supposed to be located on an arbitrarily placed planar surface. The system consists of a projector, a laptop and an uncalibrated camera. Our method is based on homography concepts and computes mappings between a camera, a projector and the region. The technique excludes calibration parameters of the camera and the projector; hence, the intrinsic and extrinsic parameters are neither given nor calculated. The positions of the projector, the camera, and the surface are unknown. For the numerous unknowns, we show that each mapping corrected distortion can be achieved. The system is capable of dynamically identifying the shape of the region of interest in which projection is on, while the region moves with a certain constant speed. Upon a sudden and abrupt motion of the region of interest, the projection iteratively adjusts its position until it fits the region perfectly. The system is demonstrated with real examples.

**Key Words**: Undistorted projection, uncalibrated camera, mobile surface projection, projector-camera system.

## 1 Introduction

Projector systems are widely used for the purpose of entertainment, work, and even as public displays. They often retain a few problems; one of the problems is a distorted projection. Unless the projector is carefully aligned with respect to the display area, the projected image appears distorted. The second problem is a fixed projection; the projector is unable to project over a mobile surface unless a special device is developed that tracks the position and orientation of the moving surface. Such problems may limit the application of a projector system. In order to solve this problem, a device like a camera can be considered to obtain the information of the position and the orientation of the surface. In this way, we can make the projection system efficient enough such that it can form an undistorted projection and project the undistorted images over a mobile surface.

There are several systems for correcting the distortion or the keystone problem of a projector as in [12], [14] and [15]. A number of systems are also designed for the integration of multiple images projected by multiple projectors to form a large seamless image as in [2], [3] and [11]. There is another research dedicated for the pose estimation of the projector using images obtained by a camera using the screen-camera homography [9]. Although these systems can provide efficient methods for projecting undistorted images on a surface, they do not handle dynamic projection. The dynamic projection includes the projection over randomly moving objects or region of interests. Another system is designed using light sensors and a frequency variation of the projector light, using a complex pre-calibration process, which needs hefty calculations and special apparatuses [8].

There exists another method for calibrating a projector using structured light patterns over the screen embedded with light sensors. This approach has two major drawbacks; first, the use of light sensors requires other communication modules to transmit necessary data to the computer; secondly the system needs to recalibrate as the position of the projection surface changes. This recalibration process is done by projecting a series of structured light patterns again [7]. Other studies have explored tracking techniques of a moving surface for projection of content; however, they primarily depend upon either electromagnetic sensors or a number of visual based tracking systems that add a significant amount of cost, infrastructure and complexity to achieve such an effect as done in [1] and [13]. Optical and magnetic trackers are used in [1] for the tracking of the projectable object while in [13] they have used photo-sensing wireless tags such as active radio-frequency (RF) tags.

In this paper, we propose a system for projection over a mobile region of interest exclusive of such complexities. Our system consists of a laptop connected to a projector and an uncalibrated camera independent of any costly sensors and trackers for the purpose of mobile projection. The mobile region of interest is supposed to be moving within a planar

* E-mail: mamonaawan@nu.edu.pk.
† E-mail: khko@gist.ac.kr.

domain, and through an image processing method the mobile region is detected and then used as a display region for projection. The image fits the moving region of interest with proper alignment, exclusive of any distortion or bleeding. The system is also capable of correcting the keystone distortion, given only a display screen is in consideration without any mobile region of interest. Our system excludes hefty calculations of calibrations of the camera, as well as the projector. The intrinsic and extrinsic elements of the projector and the camera are totally ignored and the process excludes all of such relations with these elements.

## 2 Overall Procedure

The process flow for projection over an arbitrarily placed planar surface is shown in Figure 1. The process starts by taking an image of planar surface without any projection over it via camera; the planar surface may or may not include the region of interest (ROI) at this point. This image is processed to identify the boundary of the planar surface. As the aspect ratio of the length and width of this planar surface is known, we can form a homography relation between the camera and the planar surface. We refer to this homography as $H_{cs}$ in the paper.

The second process (process 2) in Figure 1 includes projecting a source image to determine the transformation between the projector domain and the camera domain. The position of the planar surface is assumed to be such that when the source image is projected, a certain region of the source image is visible over the planar surface. An image of this projection is taken by the camera. The source image and the camera image are then used to formulate a homography relation between the projector and the camera, which is denoted as $H_{pc}$. Once these two homographies, i.e., $H_{cs}$ and $H_{pc}$ are calculated, we can form a projection over this planar surface without any distortion.

The homography relations can be summarized as:

$$\begin{pmatrix} x_p \\ y_p \\ 1 \end{pmatrix} \approx H_{pc} \begin{pmatrix} x_c \\ y_c \\ 1 \end{pmatrix} \tag{1}$$

and

$$\begin{pmatrix} x_c \\ y_c \\ 1 \end{pmatrix} \approx H_{cs} \begin{pmatrix} x_s \\ y_s \\ 1 \end{pmatrix} \tag{2}$$

In (1) and (2), $(x_p, y_p)$, $(x_c, y_c)$, and $(x_s, y_s)$ are the corresponding points in the projector domain, the camera domain, and the planar surface domain, respectively. The homography between two domains $H_{D_1 D_2}$ (where "$D_1$" and "$D_2$" represent two random domains), is an invertible 3x3 matrix. Hence, a relation between the projector and the planar surface can be formed using (1) and (2). The effect of $H_{cs}$ can be excluded from the relation calculated previously, as the relation linking the projector and the camera $H_{pc}$ is calculated using the planar surface amid. This gives us the relation between the projector and the surface as a 3x3 matrix, mathematically expressed as:

$$\begin{pmatrix} x_p \\ y_p \\ 1 \end{pmatrix} \approx {H_{cs}}^{-1} * H_{pc} \begin{pmatrix} x_s \\ y_s \\ 1 \end{pmatrix} \tag{3}$$

In Equation (3) ${H_{cs}}^{-1}$ represents the inverse of the homography $H_{cs}$.

The system then continues and determines if any region of interest is present within the planar surface or not. As shown in Figure 2, if the region of interest is absent, then the system considers the same surface as a display screen and merely

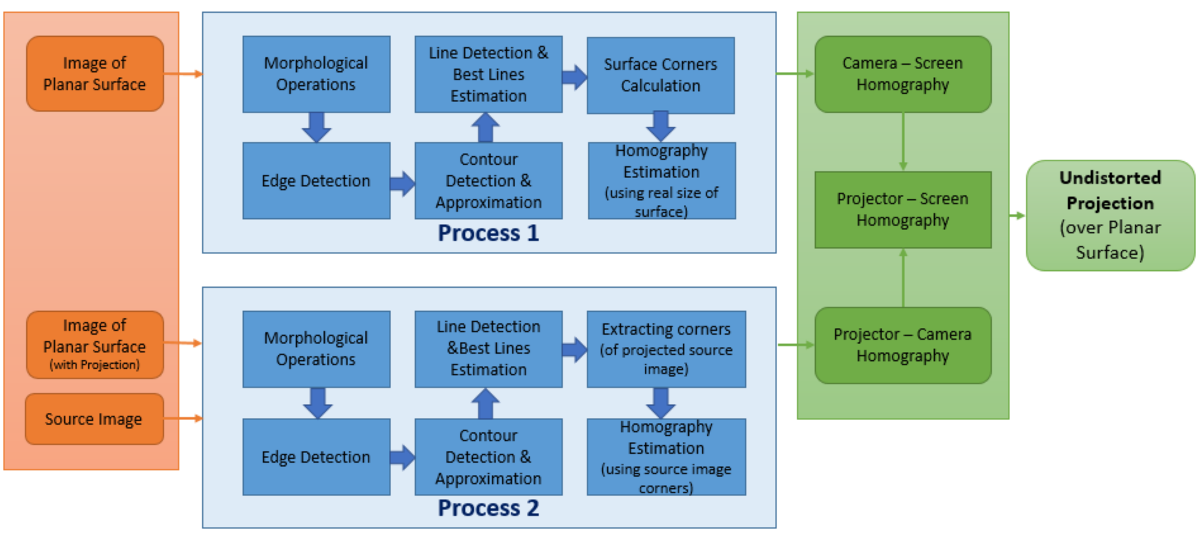


Figure 1: Process flow for projection over arbitrarily placed planar surface

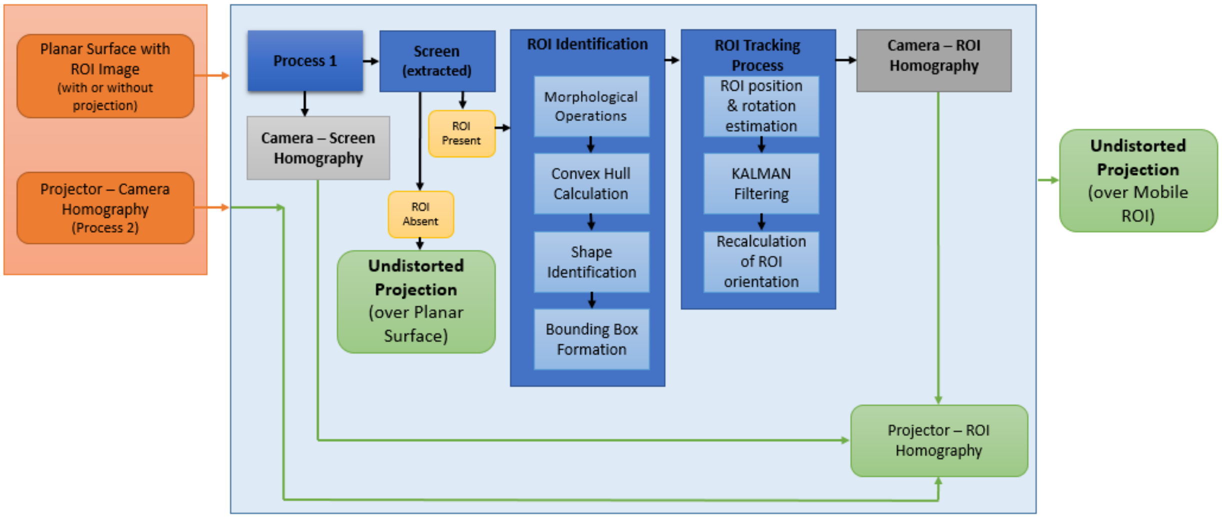


Figure 2: Process flow for projection over mobile ROI in planar surface

projects over it. If the planar surface is moved, the display modifies with respect to it as well, up to a certain extent.

If the region of interest is present, then the system follows the process flow presented further in Figure 2. It determines the position and orientation of region of interest in the surface domain. The process begins with application of morphological operations over the image that has already planar surface area extracted. Then we extract contours and form a convex hull over the contours detected. Using these contours, we identify the shape of the ROI and also form a bounding box to estimate and refine its position and orientation in the planar surface. As the original aspect ratio of the ROI is known, so we can form a homography $H_{sroi}$ for the ROI and planar surface. The expression can be stated as:

$$\begin{pmatrix} x_s \\ y_s \\ 1 \end{pmatrix} \approx H_{sroi} \begin{pmatrix} x_{roi} \\ y_{roi} \\ 1 \end{pmatrix} \tag{4}$$

Where $(x_s, y_s)$ and $(x_{roi}, y_{roi})$ are the corresponding points in the surface domain and the ROI domain respectively. $H_{sroi}$ can be used to determine the exact orientation of the ROI on the surface. The relation between the projection domain and the ROI can also be formed by using this homography. For this computation, we modify the previously calculated mapping in (3), so the mapping or homography between the ROI and a projector can be stated as:

$$\begin{pmatrix} x_p \\ y_p \\ 1 \end{pmatrix} \approx H_{sroi} * {H_{cs}}^{-1} * H_{pc} \begin{pmatrix} x_{sroi} \\ y_{sroi} \\ 1 \end{pmatrix} \tag{5}$$

$$H_{proi} = H_{sroi} * {H_{cs}}^{-1} * H_{pc} \tag{6}$$

Where $H_{proi}$ is the homography relation between the projector and the ROI. This homography can then be used to pre-warp the image to be projected such that it fits the region of interest without any distortion or bleeding. However, homography will only give us the true mapping for the ROI, so the scale and the correct position should also be considered in order to fit the projection correctly without any bleeding.

## 3 Technical Details

In order to project over the mobile surface, a few assumptions are made for our system. The mobile surface is supposed to be any of the three shapes (rectangular, triangular, or circular). It should have a white surface with black boundary to simplify identification. The system is not configured for any other shape but a few modifications can enable it to recognize other shapes as well. The shape is unknown by the system as a priori but has to be any of the above mentioned. The size of this surface is arbitrary but the aspect ratio of the length and width is assumed to be known. Only one region of interest can be introduced over the planar surface at a time. The mobile region of interest (ROI) is supposed to be moving within a planar surface. For these experiments we have taken a white board (non-reflective type) with boundaries marked with black, as a planar surface. This board can also be used as a conventional projector screen; however, its dimensions are significantly smaller as compared to a conventional projector screen. The size of screen is irrelevant and can be random; however, the aspect ratio of the size (length: width) is assumed to be known.

The tiresome task of calibrating the camera by taking pictures of a checkerboard is completely excluded; hence for any instance we do not need any intrinsic or extrinsic parameters of the camera. The relative position of the projector and the camera does not change once the system has started; however, for another instance, the relative position of the camera and the projector may vary. The experiments are performed in a projection cubicle that is a dark room with the projector being the only light source. The application is valid

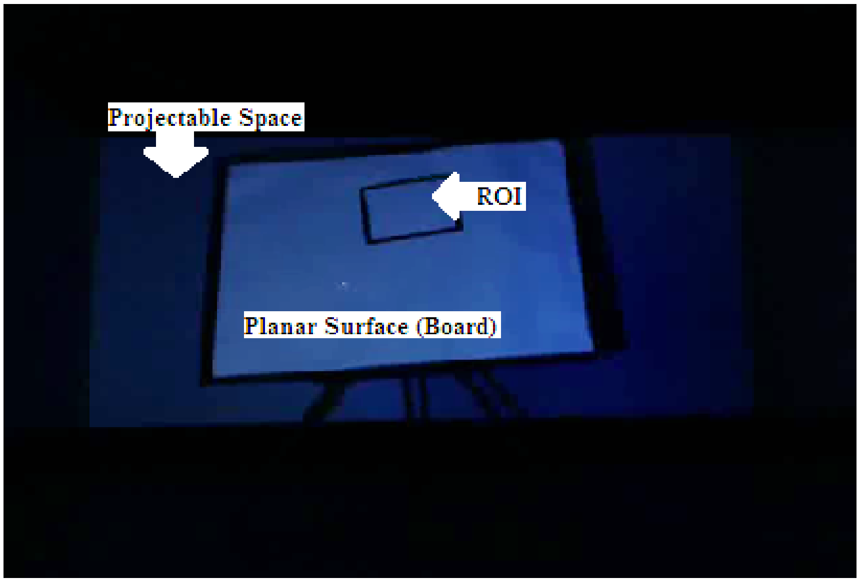


Figure 3: Planar Surface (Board) and the Region of Interest (ROI) within it, as seen by the camera. Projector (not shown) is projecting a black image to represent projectable space. The visibility of this image is improved for the sake of illustration

for most of the instances with minor changes in threshold values used in the program which can be set manually.

### 3.1 Homography Calculation

While a projection is viewed via a camera, any point in the projector domain can be mapped to a certain point in the camera domain. This mapping from the projected image to the captured image or from the captured image to the projected image, form a homograph H, a 3x3 matrix. As for any point in a domain we can calculate its corresponding point in the other domain as follows:

$$(x, y) = \left(\frac{H_{11}x' + H_{12}y' + H_{13}}{H_{31}x' + H_{32}y' + H_{33}}, \frac{H_{21}x' + H_{22}y' + H_{23}}{H_{31}x' + H_{32}y' + H_{33}}\right) \qquad (7)$$

Where (x, y) is a point in a domain and $(x', y')$ is its corresponding point in the other domain. The parameters $H_{11}$,…,$H_{33}$ are the unknowns to be determined as follows:

$$H = \begin{bmatrix} H_{11} & H_{12} & H_{13} \\ H_{21} & H_{22} & H_{23} \\ H_{31} & H_{32} & H_{33} \end{bmatrix} \qquad (8)$$

Although there are 9 unknown parameters, there are only 8 DOF (degree of freedom) as $\sum_{ij} H_{ij} = 1$. Hence, only four corresponding pairs of points are required, as each point provides two constraints. If four pairs of corresponding points are attained, then we can obtain a unique solution for these parameters by using a direct linear transformation algorithm (DLT).

**3.1.1 Camera-Planar Surface Homography**. In order to calculate camera-planar surface homography, the camera captures an image of the planar surface. This image is used to detect the boundary of the planar surface and the corners are extracted. The aspect ratio of the surface is already known. We compute the maximum length of the surface in the camera domain and calculate four corresponding points using the known aspect ratio. These corners are then used to calculate the homography "$H_{cs}$", between the camera and the surface.

We can convert each point from the surface domain to the camera domain and vice-versa using the expression stated previously in (2). If only a planar surface is provided (a planar surface does not have ROI within it), then the system uses the surface as a display screen and forms an undistorted projection over it. If the surface is moved up to some extent during this projection, the system can modify the projection simultaneously to project over it correctly; however, the main focus of the system is to project over ROI.

**3.1.2 Projector-Camera Homography**. Many techniques are followed to form a relation between a projector and a camera. These techniques usually include projecting a series of images via the projector and capturing these by the camera. The images may contain structured light patterns, AR (augmented reality) tags or even calibration grids. We exclude the cumbersome task of projecting a series of images as it takes a lot of time for a user, to project at least 10 images in the case of structured light and 3 images in the case of AR tags. We have also excluded the projection of calibration grids as it incorporates other correspondence techniques as well.

Our method includes projection of a simple image that can be reproduced without any complex considerations. The image is supposed to have a white rectangle with a black background as shown in Figure 4. It should also have dimensions similar to the resolution of the projector, so that the projector does not apply any transformation on it before projecting it. Each pixel in the image is supposed to represent each pixel in the projector domain.

The system is capable of camera exposure adjustment and the user is also given a provision to adjust the exposure, if necessary. An image of projection is taken by the camera and morphological operations are applied over it to extract the edges and register contours. These contours are then approximated into another simpler contour using the Ramer-Douglas-Puecker algorithm [10]. This approximation significantly improves the detection of lines in the contour due to reduced curves in the contour.

The lines are detected by applying Hough Lines Transform over the approximated contour and then the best fitting lines are selected using a minimum least square error computation [4]. The lines are used for the calculation of four corners of the white rectangle. These corners are then sorted in the clockwise manner and correspond with the points of the source image. The simplicity of the source image provides such convenience that we can find corresponding points in the source image by merely using a corner extraction algorithm and a sorting algorithm.

These four-point correspondences are enough for the calculation of homography $H_{pc}$.

Figure 4: The source image used for projector-camera homography calculation. The image dimensions are 1920 by 1080 pixel

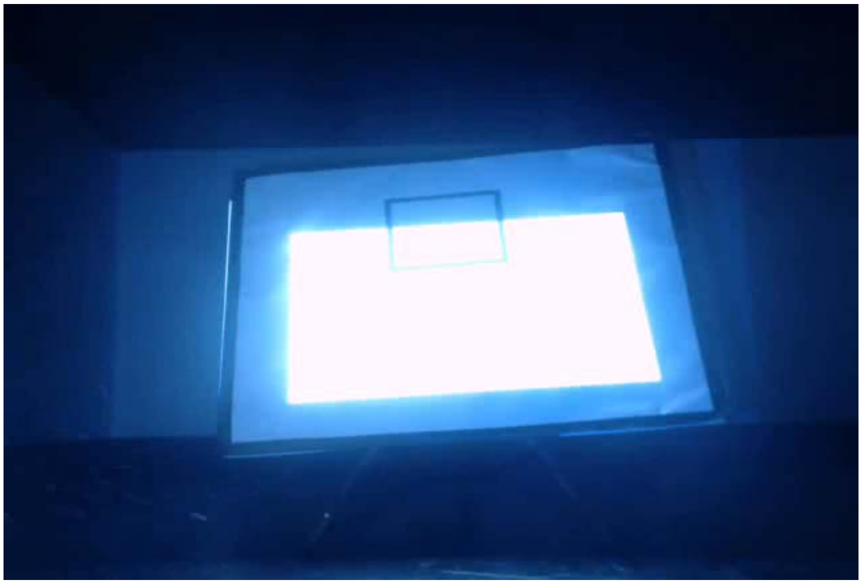

Figure 5: Projection of source image as viewed by the camera. The region of interest can also be seen in this image. The presence of ROI does not affect the calculation of projector-camera homography

Each point in the camera image or domain can be converted into the corresponding point in the projector domain using (1).

### 3.2 Initial Pose Estimation

Now that the system can already map from a projector to a camera and the camera to a planar surface, the only computation left is to form a mapping between the planar surface and the region of interest within it. For this purpose, the system analyzes the same image captured for camera-planar surface homography calculation. By applying different morphological operations, the boundary of the ROI is stored as a contour and approximated into a much simpler contour by the Ramer-Douglas-Peucker algorithm. This approximation makes it easy for us to form a better convex hull with the least computation time, as the number of vertices is significantly reduced by the approximation. This reduction in the number of vertices can be seen in Figure 6. The approximated contour also eliminates the complexity of smaller curves in the convex hull to be formed.

The convex hull is then used to identify the shape of the ROI. The vertices of the convex hull and the interior angles at each vertex are calculated along with the calculation of Hu Moments [5] of the convex hull. The number of vertices, interior angles at vertices, and Hu moments of the convex hull are the three parameters that decide the shape of the ROI. The shape of ROI can either be a rectangle, a triangle or a circle. Once the shape of ROI is decided, we form a bounding box over the convex hull of ROI. For the case of circular ROI, we form an upright bounding box (un-rotatable), as a rotatable bounding box will be redundant in this case. We form a rotatable bounding box for other shapes of ROI.

The introduction of the bounding box solves a number of problems for us. As the convex hull changes with each frame, we apply Kalman filter of order 2, over the center and the rotation angle of our corresponding bounding box [6].

The filter avoids all the abrupt changes in the position or the rotation of the bounding box and provides a smooth variation in both of these values. Furthermore, the size of convex hull also changes as each frame is processed. This variation in size is caused by different miscellaneous effects like intensity variation caused by the simultaneous projection. So, we calculate the size of the corresponding bounding box as the average of the previously determined sizes along with the recent size. Figures 6 and 7 are excellent examples to demonstrate the importance of forming a bounding box over the convex hull. Although, the convex hull in Figure 6 lacks one corner completely, the bounding box still manages to provide the fourth corner as seen in Figure 7. The corners of this bounding box can then be used to form homography $H_{sroi}$ as explained earlier in (4).

### 3.3 Image Rendering for Projection

Using the calculated mappings, we can form a pre-warp for the image to be projected; however, simply pre-warping the image will not be enough. The process of rendering the image starts by scaling the image to be projected, as homography does not give us the true scale of the image. The true scale of the image depends on the resolution of the projector, as each pixel in the image should light only one pixel in the projector domain. The system then warps the image by the inverse of $H_{proi}$ calculated in (6). The dimensions of the image to be projected are kept the same as the resolution of the projector. The image is rendered by placing the transformed image at such a position $Pos_{roi}$, that it coincides with the ROI. The rest

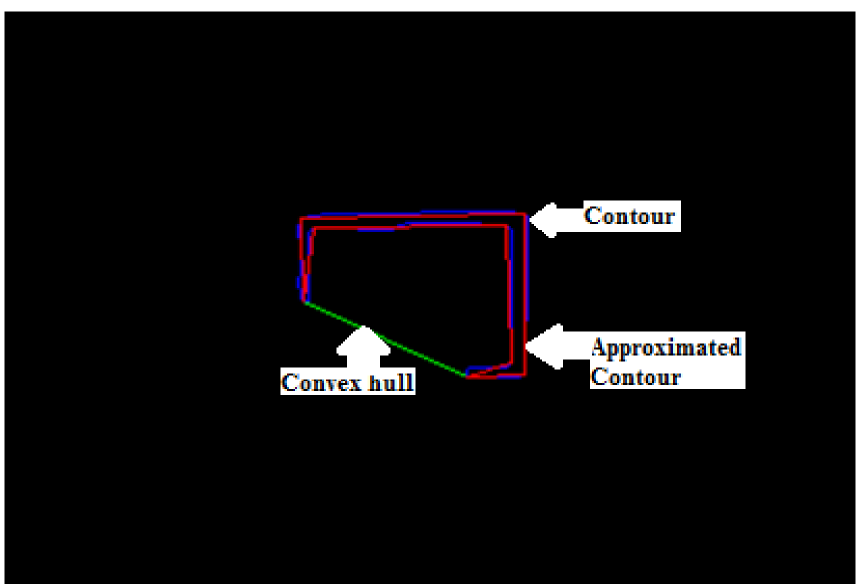


Figure 6: ROI (rectangular) is being detected in planar-surface. Contour of ROI (Blue), contour after approximation by Ramer-Douglas-Peucker algorithm (Red), and convex hull of the approximated contour (Green) can be seen in the image. The image is taken as seen in the planar surface domain

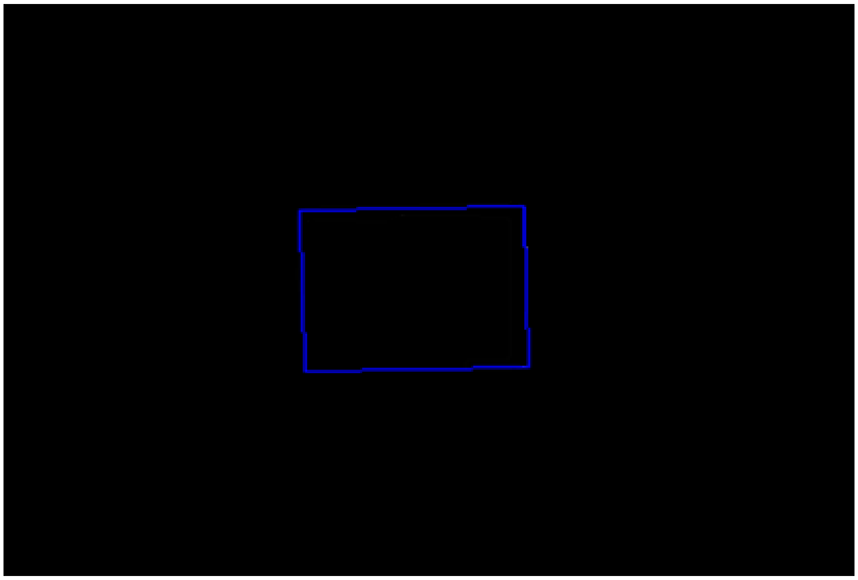

Figure 7: The bounding box for ROI (rectangular). The corresponding contours and convex hull can be seen in Figure 6. The image is shown as seen in planar-surface domain

of the pixels are rendered as black.

To calculate $Pos_{roi}$, we take in the position of ROI in planar surfaces domain and convert it into the projector domain using the inverse of $H_{proi}$. This will give us the position $Pos_{roi}$, as stated in (9).

$$Pos_{roi} = H_{proi}{}^{-1} * Pos_{sroi} \quad (9)$$

In (9), $Pos_{sroi}$ is the position of ROI as seen in the planar surface domain and $H_{proi}{}^{-1}$ represents the inverse of the mapping transformation calculated in (6). Figure 8 shows an example of the rendered image for projection.

## 4 Implementation

The projector used in our implementation is EPSON LCD Projector EB-1776W, Model H476C. The projector provides a projection at resolution of 1920 by 1080 pixels at 50-60 Hz of refresh rate. The brightness of the projector is 3000 lumens for both white and color pixels. The camera we have used is Logitech HD Pro Webcam C920 operating at 30 fps (frames per second). The webcam images are captured with the resolution of 640 by 480 pixels with a bit depth of 24. The camera also has an automatic low-light correction feature; however, this feature is disabled for these experimentations.

The application is written in C++ using OpenCV Library and implemented using a Lenovo ThinkPad E440, with Microsoft Windows 8 Pro. It has an Intel core i5-4210M processor working at 2.60GHz. The laptop has also NVidia GeForce 840M installed in it; however, GPU modules have not been used for this application. The planar surface and the region of interest both are made of a foam board, covered with a paper sheet of A0 and A4 sizes respectively.

The foam boards are considered because of their light weight and easy mobility. The boundaries of these boards are painted black. The dimensions of the foam boards for the planar surface and ROI are A0 and A4 respectively. The experiments are performed in a cubicle with only a projector as the light source. The camera is placed near the projector and the board is mounted over a poster stand. The board has an arbitrary inclination away from the setup. The distance of the board from the setup is taken to be arbitrary and has changed between different experimental instances as well.

### 4.1 Reprojection Error

As the homography we have calculated is just an approximation of the relation between the two domains, hence its projection image rendered using this approximated homography has a reprojection error. In Figure 9, the green circle represents the top-left corner of the ROI in the camera co-ordinates and the red circle represents the top-left corner of the ROI in planar surface co-ordinates. It can be vividly seen that the projected image does not coincide properly over the ROI. To solve this issue, we calculate the reprojection error in terms of Euclidean distance and then threshold it under an acceptable range. The rendered image was then modified by eliminating this error and the image overlaid over the ROI properly.

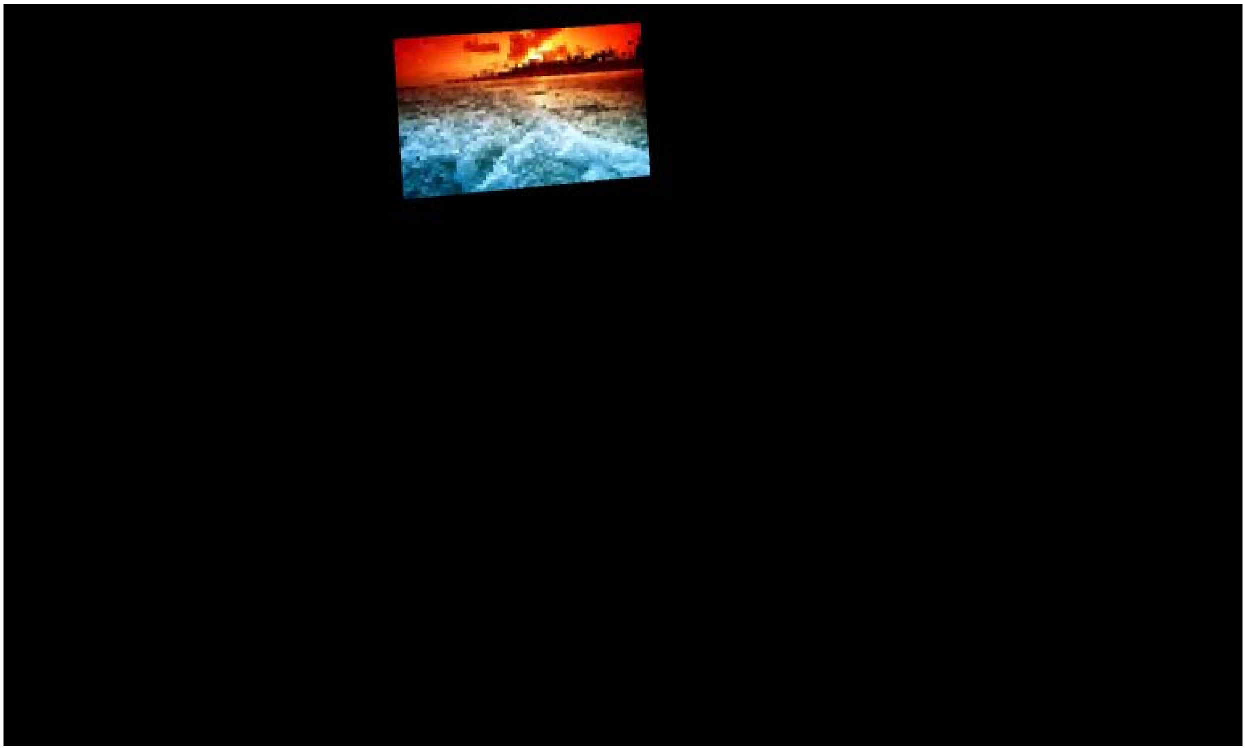

Figure 8: Sample of image rendered for projection over ROI (rectangular). The rendered image has a resolution of 1920 x1080 pixels (same as our projector)

Figure 9: The projected image does not coincide with the actual boundary

### 4.2 Image Clipping Issue

To render the image, we have used inverse transformation; however, if ROI is rotated at a larger angle then inverse transformation can cause the image to rotate out of the visible range of the of the image plane. This can result in image clipping as shown in Figure 10 where it rotates out of the ROI at the top-right corner and in Figure 11 where it rotates out at the bottom-left corner. To cater to this problem, we calculate the inverse transformation for the boundary pixels first and

Figure 10: Image clipped in top-right corner of ROI

Figure 11: Image clipped in bottom-left corner of ROI

check if those pixels are in visible range. If those pixels transform out of the visible range, we calculate the difference ($d_x, d_y$) and modify the translation of our transformation matrix. Whenever the ROI is oriented in a rotated manner, this modification allows us to refrain the clipping of the projected image.

## 5 Results

The system is tested for several instances and it takes less than 13 seconds to project and capture images. The projection converges efficiently; however, the use of a Kalman filter has significant effect over the pace of the system.

### 5.1 Planar Surface without ROI

Figure 12 shows an image being displayed over the planar surface without any keystone distortion or bleeding. As ROI is absent, the system utilizes whole planar surfaces to display the image. The system also effectively forms a correct projection over the planar surface even if it is moved up to an extent. The orientation of the surface has also changed for various instances. This difference can be observed clearly in Figures 12, 13, 14, and 15.

Figure 12: Planar surface is used a display screen, while ROI is not provided. The projection is keystone corrected and does not bleed out of the planar surface

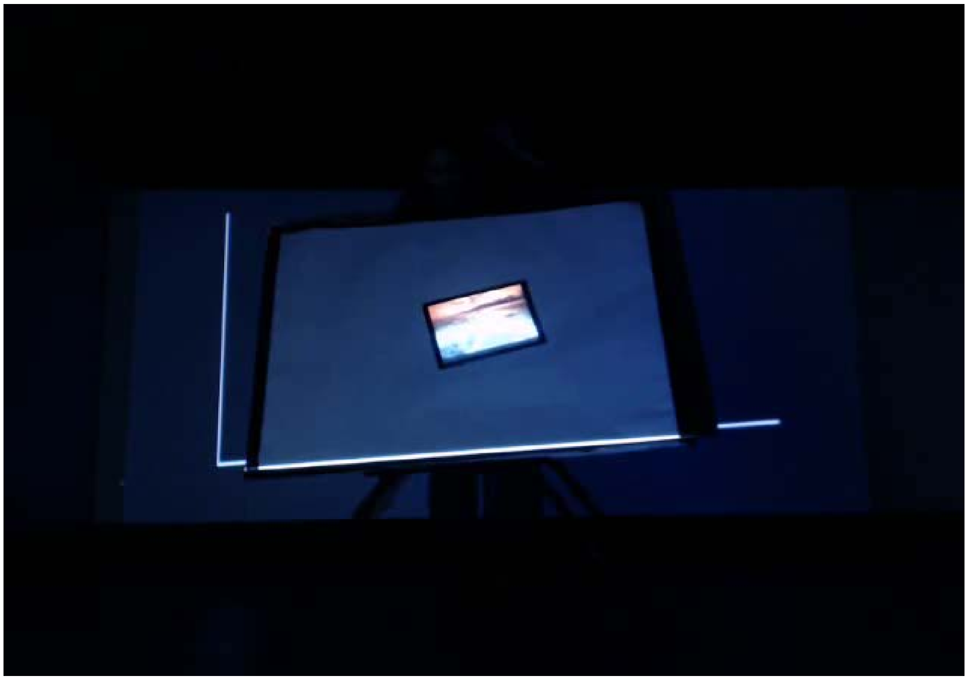

Figure 13: Projection fits the rotated rectangular ROI with proper orientation and position precisely. The illuminated lines are boundaries of window displaying the image

### 5.2 Planar Surface with ROI

The projection image modifies as soon as the ROI is moved and fits over it correctly provided that the ROI is moved with a constant speed and there are no sudden changes or movements. If the ROI is moved abruptly, the projection follows it, and then oscillates about it while the distance error between the current position and the required position decreases. The oscillations of the projection finally converge to the correct position of the ROI for all the instances.

Figures 14 and 15 illustrate the occasions where the system has successfully formed a precise projection over a triangular and a circular ROI, respectively. For the case where the ROI is abruptly moved from an extreme corner to the other extreme corner, the setting time or convergence time for the projection is calculated to be 5 seconds on the average.

Figure 13 shows the projection over rectangular ROI, where the projection image can be seen perfectly fitted over the ROI, even though the ROI has significantly larger angle of rotation. The illuminated lines in Figures. 13, 14, and 15, are the boundaries of the window containing the rendered image. The resolution of the rendered image can also be adjusted to eliminate these lines; however, the concern of this application is not affected by them.

During these experiments, we moved the ROI abruptly to test its efficiency. The system successfully fits the projection after a few oscillations upon abrupt motion. It is also moved with a constant speed while the projection fits over it perfectly.

## 6 Discussion

The results of this approach can be improved by introducing fast computing techniques such as the use of GPU and a camera with a better frame per second rate. As we used a webcam, an addition of a camera with better resolution will provide considerably precise information.

The accuracy of the system can yet be improved by taking more images while forming homography mappings. The homography with a least re-projection error can be selected from the homographies calculated using these images. However, these benefits come with a significant cost of either time or expenditure.

A cell phone application version of this system is also being considered to be designed. The cell phone application will utilize the in-built camera of the cell phone and a Pico projector will be required, to be connected with the cell phone via a data cable. Such a system will have an exceptional portability, as cell phones and Pico projectors are sufficiently compact and easily portable.

## 7 Conclusion

We have designed a simple system for projection over a mobile region of interest by using an uncalibrated camera. The system tracks and projects over the region of interest with true orientation and scale, while the region of interest moves with a certain constant speed. It takes minimal information to form

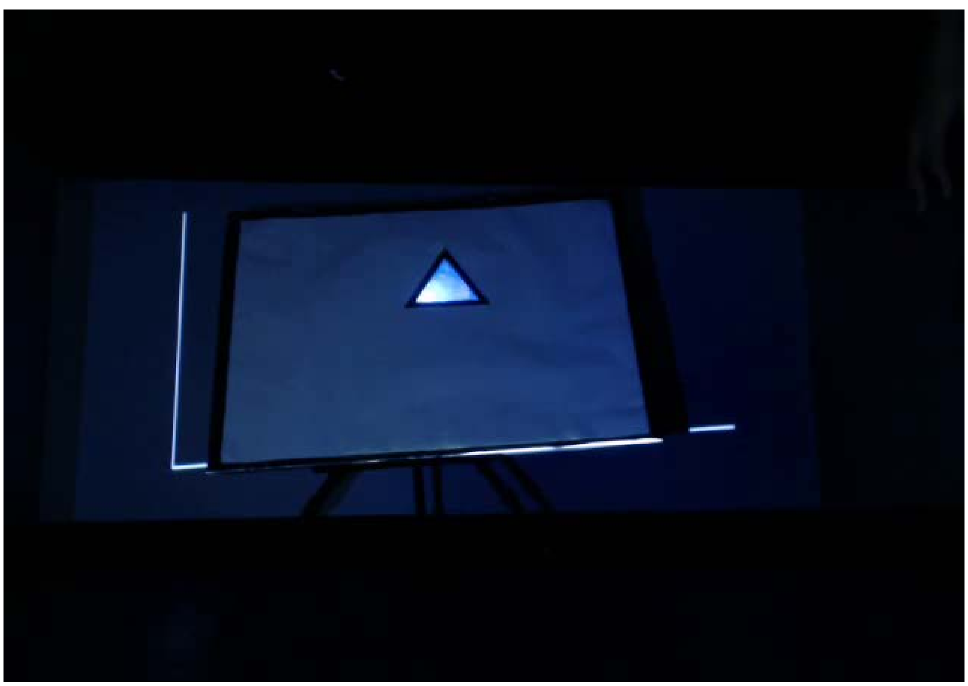

Figure 14: Triangular ROI is introduced over the planar surface. The system identifies the shape and projects over it, while it moves in the planar surface

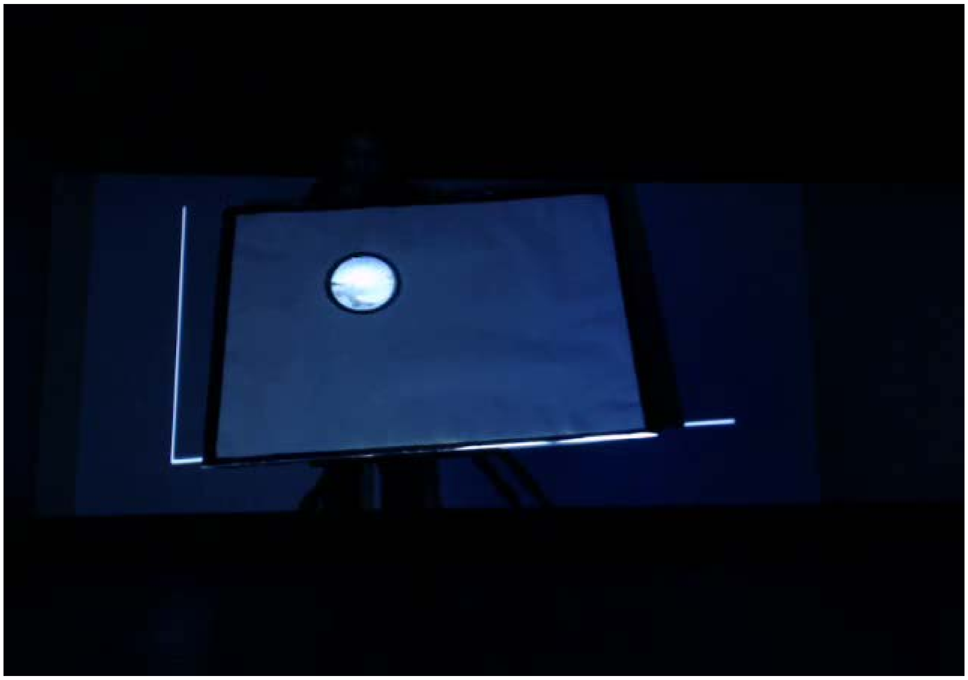

Figure 15: The instance of circular ROI with image projected over it. The projection for this complex shaped ROI overlays entirely without any bleeding

homographies between a projector, an uncalibrated camera, and the planar surface with ROI in it. The system is provided with no information about the intrinsic and extrinsic parameters and neither calculates them. It is assessed to be efficient enough for projection over the ROI without bleeding out of it. As other researches depend over specialized equipment to track the mobile projection area, our system excludes all such specialized apparatuses and equipment. Our system can also utilize the in-built camera of the laptop or even of a cell phone for this purpose, making it suitable for common use.

### References


[1] D. Badyopadhyay, R. Raskar, and H. Fuchs, "Dynamic Shader Lamps: Painting on Real Objects", IEEE ACM Int. Symposium on Augmented Reality (ISAR), New York, 2001.

[2] M. Beus, R. Blach, S. Stegmaier, and U. Hafner, "Towards a Scalable High-Performance Application Platform for Immersive Virtual Environments", Eurographics Workshop on Virtual Environments, 2001.

[3] C. Cruz-Neira, D. J. Sandin, T. A. DeFanti, R. Kenyon, and J. C. Hart, "The CAVE, Audio Visual Experience Automatic Virtual Environment", Communications of the ACM, pp. 64-72, 1992.

[4] P. V. C. Hough, "Machine Analysis of Bubble Chamber Pictures", *Proc. Int. Conf. High Energy Accelerators and Instrumentation*, pp. 554-558, 1959.

[5] M. K. Hu, "Visual Pattern Recognition by Moment Invariants", *IRE Transactions of Information Theory*, pp. 179–187, 1962.

[6] R. E. Kalman, "A New Approach to Linear Filtering and Prediction Problems", *Transactions of the ASME – Journal of Basic Engineering*, pp. 34-45, 1960.

[7] J. C. Lee, P. H. Dietz, D. Aminzade, and S. E. Hudson, "Automatic Projector Calibration using Embedded Light Sensors", *Proc. ACM UIST '04*, pp. 123-126, 2004.

[8] J. C. Lee, S. E. Hudson, J. W. Summet, and P. H. Dietz, "Moveable Interactive Projected Displays Using Projector Based Tracking", *Proc. ACM UIST '05*, pp. 63-72, 2005.

[9] T. Okatani, and K. Deguchi, "Autocalibration of a Projector-Camera System", *IEEE Transactions of Pattern Analysis and Machine Intelligence* 27(12):1845-1855, 2005.

[10] U. Ramer, "An Iterative Procedure for the Polygonal Approximation of Plane Curves", *Computer Graphics and Image Processing* 1(3):244-256, 1972.

[11] R. Rasker, M. S. Brown, R. Yang, W. C. Chen, G. Welch, and H. Towles, "Multi-Projector Displays Using Camera-Based Registration", *Proc. IEEE Visualization*, pp. 161-168, 1999.

[12] R. Raskar, P. A. Beardsley, "A Self-Correcting Projector", IEEE Computer Society Conference on Computer Vision and Pattern Recognition (CVPR), pp. II-504-II-508 2001.

[13] R. Raskar, P. A. Beardsley, J. V. Baar, Y. Wang, P. H.

Dietz, J. Lee, D. Leigh, and T. Willwacher, "RFIG Lamps: Interacting with a Self-Describing World via Photosensing Wireless Tags and Projectors", *Proc. of ACM SIGGRAPH*, 23(3):406-415, 2004.

[14] R. Suthankar, R. Stockton, and M. Mulin, "Automatic Keystone Correction for Camera-Assisted Presentation Interfaces", *Proc. International Conference on Multimodal Interfaces (ICMI)*, pp. 607-614, 2000.

[15] R. Suthankar, R. Stockton, and M. Mulin, "Smarter Presentations: Exploiting Homography in Camera-Projector Systems", *Proc. International Conference on Computer Vision*, pp. 247-253, 2001.

**Mamona Awan** received Bachelor's degree in Mechatronics and Control Engineering from University of Engineering and Technology, Lahore Pakistan in 2013. She did Masters in Mechatronics from Gwangju Institute of Science and Technology, South Korea in 2016. She has also worked as a research assistant in School of Mechatronics (GIST, South Korea). She is currently a lecturer in National university of Emerging Sciences-FAST, Lahore Pakistan. She has research experience in Computer Vision, Computer Graphics and Spatial Augmented Reality. Her research interests include computer vision, graphics, augmented reality, 3D modeling and robotics.

**Kwang Hee Ko** received a B.S degree in Naval Architecture and Ocean Engineering from Seoul National University in 1995, M.S. degrees in Mechanical and Ocean engineering in 2001 and a Ph.D. degree in Ocean Engineering from the Massachusetts Institute of Technology (MIT), Cambridge, MA, USA, in 2003. His research interests include automation of ship and offshore fabrication, feature matching, landmine detection, geometric modeling, CAD/CAM and computer graphics. He worked as a postdoctoral associate at MIT from 2003 to 2004 and as a research associate at the Design and Manufacturing Institute, Stevens Institute of Technology, Hoboken, NJ, from 2004 to 2005. He joined the School of Mechanical Engineering, Gwangju Institute of Science and Technology, Gwangju, Korea, in 2006 and worked as an assistant professor until 2010 and as an associate professor until 2016. He is currently a professor at the Gwangju Institute of Science and Technology, Gwangju, Korea.